

Multiscale modeling of stress-mediated diffusion in silicon: *Ab initio* to continuum

Matthew Laudon, Neil N. Carlson, and Michael P. Masquelier

Computational Materials Group at Los Alamos National Laboratory, Motorola, Inc., MS B285, Los Alamos, New Mexico 87545

Murray S. Daw and Wolfgang Windl^{a)}

Computational Materials Group, Motorola, Inc., Austin, Texas 78721

(Received 26 September 2000; accepted for publication 6 November 2000)

In this letter, we present the development of a complete methodology to simulate the effects of general anisotropic nonuniform stress on dopant diffusion in silicon. The macroscopic diffusion equation is derived from microscopic transition-state theory; the microscopic parameters are calculated from first principles; a feature-scale stress-prediction methodology based on stress measurements in the relevant materials as a function of temperature has been developed. The developed methodology, implemented in a continuum solver, is used to investigate a TiN metal gate system. A compressive stress field is predicted in the substrate, resulting in an enhancement in lateral boron diffusion. This enhancement, which our model attributes mostly to solubility effects, is in good agreement with experiment. © 2001 American Institute of Physics.
[DOI: 10.1063/1.1336158]

Traditionally, it has been assumed that the major effect of substrate stresses were dislocation formation and response,^{1,2} whereas stress effects on diffusion were thought to be negligible.³ With the reduction of gate lengths and the use of more exotic gate materials, stress-mediated diffusion becomes a more prevalent component in determining the final dopant profile and subsequent device performance. On the experimental side, contradictory results for the qualitative influence of stress on boron diffusion further motivate a fundamental investigation of stress-mediated diffusion. While the measurements of Aziz and co-workers suggest enhanced diffusivity under compressive pressure,^{4–6} other works find retarded diffusion in that case.^{3,7–9} Hence, this letter focuses on the effect of stress on B diffusion in Si.

Most existing theoretical work on stress-mediated diffusion assumes hydrostatic stress in the substrate. However, stresses caused by dislocations, thermal processes, and geometric effects all add to a complex stress state under a multilayered gate stack—where the gate itself acts as a stress concentrator—with magnitudes approaching the material strength even at low temperatures.^{3,10–12} Since the only previous derivation¹³ of the diffusivity in a general stress field from atomic hopping rates was restricted to special cases that did not include diffusion on a diamond lattice, we extended the theory to the general case which will be given in more detail elsewhere.¹⁴

Boron has been found to diffuse nearly exclusively with the help of Si self-interstitials.¹⁵ Using *ab initio* calculations, a two-step diffusion mechanism has been recently identified for the mobile BI pair [see Fig. 1(a) or 1(c)].¹⁶ The intermediate hexagonal interstitial [Fig. 1(b)] is a saddle point for the positive, and a local minimum close to the saddle point

for the neutral charge state, and is assumed to be the dominant saddle point in *p*-type Si in this letter.

A standard four-stream diffusion model for B consists of the streams *I* (self-interstitials, mobile), *V* (vacancies, mobile), *B* (substitutional B, immobile), and *BI* (B–interstitial pair, mobile). Conjecturing that the point defects (*I* and *V*) are in equilibrium with a free surface and that the *I* concentration is independent of the *B* concentration, we can simplify the four-stream model to an effective one-stream model,

$$\frac{\partial C_B}{\partial t} = \nabla \cdot [\mathbf{P}_B^{\text{eff}} \nabla (C_B / S_B^{\text{eff}})], \quad (1)$$

where C_B is the B concentration, $\mathbf{P}_B^{\text{eff}}$ is the effective solid permeability tensor, and S_B^{eff} is the solid solubility factor.¹⁴ In the hydrostatic case where the stress tensor $\boldsymbol{\sigma}$ is given by $\boldsymbol{\sigma} = p \mathbf{Id}$, the permeability (which is a scalar now) as a function of the pressure *p* is given by

$$P_B^{\text{eff}} = P_{BI} = D_B^0 \exp\left(-\frac{\epsilon_s^{BI} + p\Omega_s^{BI}}{k_B T}\right), \quad (2)$$

where D_B^0 is the diffusivity prefactor for intrinsic B diffusion, which we calculate from first principles within the harmonic Vineyard method,¹⁷ ϵ_s^{BI} is the creation energy for the BI pair at the saddle point, Ω_s^{BI} is the corresponding creation

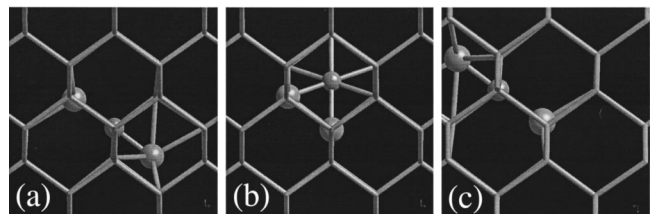


FIG. 1. Diffusion path for B as determined from *ab initio* calculations (see Ref. 16). The smaller ball is the B atom.

^{a)}Electronic mail: wolfgang.windl@motorola.com

volume,¹⁸ k_B is the Boltzmann constant, and T the temperature. “Creation” quantities are equivalent to formation quantities defined with respect to perfect Si as a reference system.¹⁴ For the solubility, we find

$$S_B^{\text{eff}} = \exp \left[- \frac{\varepsilon_v^B + \varepsilon_{\text{at}} + p(\Omega_v^B + \Omega_{\text{at}})}{k_B T} \right], \quad (3)$$

where ε_v^B is the creation volume for substitutional B in its ground state or “valley,” ε_{at} is the total energy per atom of the perfect Si cell, Ω_v^B is the corresponding creation volume for substitutional B, and Ω_{at} the volume per atom of perfect Si.¹⁸ For the anisotropic case with general stress tensor, the expressions are more complicated and will be given elsewhere.¹⁴

The general stress dependence is given by the respective creation volume tensors which are calculated by the length changes ΔL_α between the defective cell and the perfect Si cell with lattice parameters L_α , $\Omega = (\Omega)_{\alpha\beta} = \delta_{\alpha\beta} \varepsilon_{\alpha\gamma\delta} \Delta L_\alpha L_\gamma L_\delta$ in a principal-axes system. Since the single elements of the volume tensors are hard to separate experimentally, we calculate them from first principles. Although several *ab initio* investigations examined the (scalar) hydrostatic pressure dependence of diffusion in the past,^{19,20} there is no previous report on the corresponding tensor dependence for the general anisotropic stress case in the literature.

Using the *ab initio* code VASP,²¹ within the generalized-gradient approximation, we find from supercell calculations of up to 1000 atoms that the finite-size change of the bulk modulus of the defective cell can strongly influence the results. This error needs to be corrected for smaller systems, which can be done easily. Band-gap and finite-size corrections are applied to the energy values; further details can be found elsewhere.¹⁸

We calculate $\varepsilon_v^B + \varepsilon_{\text{at}} = -7.14$ eV and $\varepsilon_s^{Bf} = -3.39$ eV, which results in a net activation energy of $E_a = -(\varepsilon_v^B + \varepsilon_{\text{at}}) + \varepsilon_s^{Bf} = 3.75$ eV in good agreement with the experimental value of Ref. 22. Furthermore, we find $(\Omega_s^{Bf})_{\alpha\beta} = \delta_{\alpha\beta} [9.5\delta_{\alpha x} - 3.8(\delta_{\alpha y} + \delta_{\alpha z})]$ \AA^3 in a principal-axis system with the x axis parallel to the (111) direction and $\Omega_v^B + \Omega_{\text{at}} = 2.4 \mathbf{Id}$ \AA^3 , respectively, with scalar values for the hydrostatic case of $\mathbf{Tr}(\Omega_s^{Bf}) = 1.9 \text{\AA}^3$ and $\mathbf{Tr}(\Omega_v^B + \Omega_{\text{at}}) = 7.2 \text{\AA}^3$. The net scalar activation volume is $V_a = -\mathbf{Tr}(\Omega_v^B + \Omega_{\text{at}}) + \mathbf{Tr}(\Omega_s^{Bf}) = -5.3 \text{\AA}^3$, in good agreement with recent experiments⁵ of -3.4\AA^3 and isotropic *ab initio* calculations²⁰ of -3.1\AA^3 . Although the hydrostatic value is small, there is considerable anisotropy in the permeability volume tensor which can have a significant effect on diffusion under anisotropic strain.¹⁴ Our results suggest that in the considered equilibrium case B diffusion is *enhanced* by compressive pressure. This is mostly a solubility effect and, in consequence, due to the fact that our point defects are in equilibrium with a free surface.¹⁸

A titanium nitride (TiN) metal gate integration on a sub-quarter micron p -metal–oxide–semiconductor field-effect transistor is used as a demonstration example of the stress-diffusion phenomena, where anomalous stress-dependent boron diffusion has been recently discovered at Motorola.¹² Electrically measured lateral diffusion results indicated an enhancement in boron diffusion with increasing gate stress.

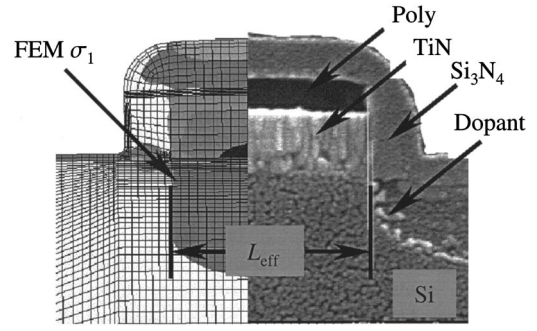


FIG. 2. Scanning electron microscope image (see Ref. 12) and finite-element model of the TiN gate stack of Ref. 12.

Figure 2 shows an example of a scanning electron microscope image of the gate along with a feature scale stress model.

A finite-element method is used to predict high-temperature feature scale stresses in the Si substrate under the TiN metal gate. Since the temperature dependence of elastic properties for most materials in a gate stack, except for Si, is unknown, empirical data are used to calibrate the high-temperature stress simulations. A full three-dimensional (3D) finite-element model had to be used, since plane-strain and plane-stress two-dimensional (2D) reductions are insufficient in the area of interest near the Si surface. A 100 \AA SiO₂ film was modeled over the gate in order to reduce the potential singularity found in finite-element peeling stress results near free-traction boundaries.¹¹ The TiN has a high tensile stress at anneal temperatures (1025 $^\circ\text{C}$), resulting in compressive horizontal stresses directly under the gate and large compressive and tensile stress concentrations just under and outside the gate edge, respectively.

Resulting 3D stress tensors from the finite-element model are passed through nodal data to an in-house stress diffusion solver (MANIFEST) that is based upon the partial differential equation solver described in Ref. 23. This solver employs the gradient-weighted moving finite-element method which uses a continuously moving mesh that adapts to the evolving solution. The diffusion equation implemented on our solver is

$$S_B^{\text{eff}} \frac{\partial w}{\partial t} = \nabla \cdot \mathbf{P}_B^{\text{eff}} \nabla w + \nabla w \cdot \mathbf{P}_B^{\text{eff}} \nabla w, \quad (4)$$

where the transformed variable $w = \log(C_B/S_B^{\text{eff}})$ was introduced in order to achieve a relative accuracy in the concentration tail comparable to that in the high-concentration regions. Galerkin equations are obtained by minimizing the residual of this equation with respect to a $1/S_B^{\text{eff}}$ weighted L^2 norm. At present the stress tensor, upon which S_B^{eff} and $\mathbf{P}_B^{\text{eff}}$ depend, is simply obtained by interpolating the finite-element-computed stress field onto the moving mesh. Using the described procedure, postanneal diffusion profiles for the TiN metal gate as well as for a reference stress-free gate are calculated.

The resulting profiles for a 5 keV implanted B profile diffused at 1025 $^\circ\text{C}$ for 10 s can be seen in Fig. 3. Due to stress effects, an 8% change in L_{eff} for a 250 nm L_{drawn} device is predicted. Equivalently, a 30% change in L_{eff} is predicted for a 65 nm L_{drawn} device. These numbers are

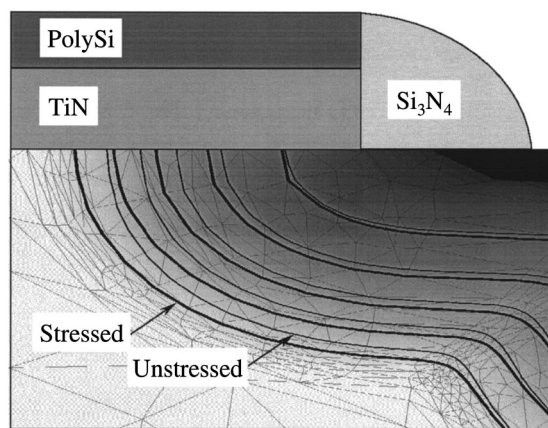


FIG. 3. Boron concentration contours for a 10 s, 1025 °C, boron diffusion (source/drain+extension). Comparison of the TiN metal gate stressed case (heavy line) to a unstressed (light line) solution show a 8% difference in lateral diffusion for a 250 nm L_{drawn} gate.

quantitatively in good agreement with the experimental findings, which possibly suggests the reasonability of the basic assumption in our model, i.e., the use of an equilibrium one-stream model which does not allow for transient-enhanced diffusion or B clustering effects. This might be caused, e.g., by a possible nature of the interface (or other extended defects) as a fast sink for point defects which could reinstate the equilibrium concentrations of the point defects quickly and allow the solubility to dominate the pressure dependence of the diffusivity. If this were true, it might also give an explanation for the qualitative difference between the above-mentioned measurements, assuming they are correct: In cases where *enhanced* B diffusion is found under compressive stress,^{4–6} the point defect concentrations in the system would be in equilibrium with the free surfaces. For the opposite case,^{3,7–9} this equilibrium might be disturbed because of, e.g., interactions of the point defects with defects other than free surfaces, which might suppress the solubility effect and result in *retarded* B diffusion under compressive stress.

In summary, we described in this letter the development of a complete methodology to simulate the effects of general anisotropic nonuniform stress on diffusion of B in Si. This methodology includes the derivation of the macroscopic diffusion equation from microscopic transition state theory, calculation of the required microscopic parameters from first principles, development of a feature-scale stress-prediction methodology based on measurements of the stress in the gate stack materials as a function of temperature, and final implementation into a continuum model. For the investigated case of an advanced metal gate system, significant stress effects on B diffusion were predicted which strongly corroborate

with Motorola's metal gate experimental results.¹² Our results suggest a possible explanation for the qualitative difference between experiments by pointing out the crucial role of the equilibrium of the point defects with free surfaces. Furthermore, our findings imply the possibility to control excessive B diffusion by using a different gate metal that causes tensile instead of compressive stress in the substrate which should slow down B diffusion.

The authors thank Bikas Maiti and Jeff Cheng from Motorola and Mike Aziz from Harvard for very helpful discussions.

¹P. Kuo, Appl. Phys. Lett. **66**, 580 (1995).

²Y. Zaitzu, K. Osada, T. Shimizu, S. Matsumoto, M. Yoshida, E. Arai, and T. Abe, Mater. Sci. Forum **196–201**, 1891 (1995).

³H. Park, K. S. Jones, J. A. Slinkman, and M. E. Law, J. Appl. Phys. **78**, 3664 (1995).

⁴M. Aziz, Defect Diffus. Forum **153–155**, 1 (1998); Y. Zhao, M. Aziz, S. Mitha, and D. Schiferl, Appl. Phys. Lett. **74**, 31 (1999).

⁵Y. Zhao, M. Aziz, H.-J. Gossmann, S. Mitha, and D. Schiferl, Appl. Phys. Lett. **75**, 941 (1999).

⁶Y. Zhao, M. Aziz, H.-J. Gossmann, and S. Mitha, Appl. Phys. Lett. **74**, 31 (1999).

⁷S. Chaudhry and M. E. Law, J. Appl. Phys. **82**, 1138 (1997).

⁸K. Osada, Y. Zaitzu, S. Matsumoto, M. Yoshida, E. Arai, and T. Abe, J. Electrochem. Soc. **142**, 202 (1995).

⁹Y. Todokoro and I. Teramoto, J. Appl. Phys. **49**, 3527 (1978).

¹⁰E. Suhir, J. Appl. Mech. **55**, 143 (1988); D. B. Bogy, *ibid.* **35**, 460 (1968).

¹¹B. Gu and P. E. Phelan, Appl. Supercond. **6**, 19 (1998).

¹²B. Maiti, P. J. Tobin, C. Hobbs, R. I. Hegde, F. Huang, D. L. O'Meara, D. Jovanovic, M. Mendicino, J. Chen, D. Connelly, O. Adetutu, J. Mogab, J. Candelaria, and L. B. La, Tech. Dig. Int. Electron Devices Meet. 781 (1998).

¹³P. H. Dederichs and K. Schroeder, Phys. Rev. B **17**, 2524 (1978).

¹⁴M. S. Daw, W. Windl, M. Laudon, N. N. Carlson, and M. P. Masquelier (unpublished).

¹⁵See, e.g., A. Ural, P. B. Griffin, and J. D. Plummer, Phys. Rev. Lett. **83**, 3454 (1999), and references therein.

¹⁶W. Windl, M. M. Bunea, R. Stumpf, S. T. Dunham, and M. P. Masquelier, in *Proceedings of the Second International Conference on Modeling and Simulation of Microsystems*, April 19–21, 1999, San Juan, Puerto Rico (Computational Publications, Cambridge, MA, 1999), p. 369; Phys. Rev. Lett. **83**, 4345 (1999).

¹⁷B. P. Uberuaga, R. Stumpf, W. Windl, H. Jonsson, and M. P. Masquelier (unpublished); this work also finds that stress effects on prefactors are small compared to exponential effects, hence we neglect the former.

¹⁸W. Windl, M. S. Daw, M. Laudon, N. N. Carlson, and M. P. Masquelier (unpublished).

¹⁹See, e.g., A. Antonelli and J. Bernholc, Phys. Rev. B **40**, 10643 (1989); A. Antonelli, E. Kaxiras, and D. J. Chadi, Phys. Rev. Lett. **81**, 2088 (1998).

²⁰B. Sadigh, T. J. Lenosky, S. K. Theiss, M.-J. Caturla, T. Diaz de la Rubia, and M. A. Foad, Phys. Rev. Lett. **83**, 4341 (1999).

²¹G. Kresse and J. Hafner, Phys. Rev. B **47**, 558 (1993); G. Kresse and J. Furthmüller, Comput. Mater. Sci. **6**, 15 (1996); Phys. Rev. B **54**, 11 169 (1996).

²²Y. M. Haddara, B. T. Folmer, M. E. Law, and T. Buyuklimanli, Appl. Phys. Lett. **77**, 1976 (2000).

²³N. N. Carlson and K. Miller, SIAM J. Sci. Comput. (USA) **19**, 728 (1998); **19**, 766 (1998).